Water Resources Management (2023) 37:5343–5366
https://doi.org/10.1007/s11269-023-03610-0

Investigating the Effect of Spatial and Temporal Variabilities of Rainfall on Catchment Response

Pardis Ziaee[1] · **Mohammad Javad Abedini**[1]

Received: 10 June 2023 / Accepted: 4 September 2023 / Published online: 30 September 2023

Abstract
This study investigates the influence of rainfall variability in time and space, as well as the location of storm center, on catchment outflow hydrograph. Synthetic data of over 600 rainfall events were generated for the Walnut Gulch catchment in Arizona using two rainfall generation models. After calibrating the distributed MIKE-SHE rainfall-runoff model for a sub-catchment in the basin, we subsequently used it to simulate the entire catchment behavior by employing the generated synthetic rainfall data with predetermined characteristics. The findings demonstrate that the storm center location has a significant impact on the characteristics of the outflow hydrograph, with closer proximity to the outlet resulting in increased peak magnitude and decreased time to peak. The spatiotemporal resolution of the monitoring network also affects the hydrograph characteristics, particularly the peak magnitude, with lower resolutions leading to underestimation of peak and overestimation of time to peak. The impact of spatial resolution on hydrograph characteristics increases as the correlation of rainfall events in space decreases. However, the effect of rainfall temporal resolution on catchment response remains almost consistent regardless of temporal correlation. Ultimately, the results imply that accurate estimation of the outflow hydrograph requires a monitoring network with relatively high spatial and temporal resolutions.

Keywords Rainfall temporal variability · Rainfall spatial variability · Stochastic rainfall generation · MIKE System Hydrological European (MIKESHE)

1 Introduction

Floods are one of the most costly and deadliest natural disasters, annually affecting tens of millions of lives and causing catastrophic damage worldwide. Despite higher absolute economic losses from flooding in developed countries, it is observed that developing countries have always experienced the highest fatality rates and economic losses associated with floods (Singh 2016). Consequently, gaining more knowledge about the flood-related processes, particularly by introducing various synthetic scenarios (e.g., synthetic rainfall input) into physically-based rainfall-runoff models, to come up with applicable flood mitigation methods and

✉ Mohammad Javad Abedini
abedini@shirazu.ac.ir

[1] Department of Civil and Environmental Engineering, Shiraz University, Shiraz, Iran

develop reliable flood forecasting and warning systems, has always been an important research agenda among the hydrologists in different countries (Blöschl et al. 2019).

Rainfall exhibits significant variabilities in both time and space (Carvalho and Woodroffe 2015). These variations have been identified as the primary source of uncertainty in rainfall-runoff models and flood forecasting (Beven 2012; Lin et al. 2022). This might explain why nearly 50% of the 23 unanswered questions in hydrological sciences journal concern with the spatial and temporal variabilities in the processes of the hydrological cycle (Blöschl et al. 2019). Therefore, understanding the impact of spatiotemporal variations in rainfall input on catchment response is crucial, as inconsistent findings in the existing literature necessitate a thorough investigation into the influence of these variabilities on hydrologic response.

A review of the literature on the effect of rainfall spatial characteristics on catchment response reveals varied approaches employed by researchers. Several scholars have examined the influence of rainfall monitoring network density, encompassing both ground-based and remotely-sensed data, on outlet hydrograph (Bell and Moore 2000; Hohmann et al. 2021; Krajewski et al. 1991; Lobligeois et al. 2014; Lopes 1996; Meselhe et al. 2009; Ochoa-Rodriguez et al. 2015; Rafieeinasab et al. 2015; Schuurmans and Bierkens 2007; Senan et al. 2022; Terink et al. 2018). Others have made efforts to ascertain the impact of the coefficient of variation of precipitation fields on catchment response (Caracciolo et al. 2014; Zhang and Han 2017; Zhang et al. 2018). Additionally, certain investigators have explored how the spatial correlation of precipitation fields affects the surface runoff characteristics (Paschalis et al. 2014; Wilson et al. 1979). Eventually, numerous studies have been dedicated to the effect of spatial patterns of the precipitation field and storm center location on outlet hydrograph characteristics (Beven and Hornberger 1982; Chen et al. 2023; Nicótina et al. 2008; Younger et al. 2009). Despite the broad literature on the relationship between spatial characteristics of rainfall and the catchment response, the conclusions have been conflicting. This is particularly evident when considering factors such as the size of the catchment under investigation (Michaud and Sorooshian 1994; Nicótina et al. 2008; Segond et al. 2007; Zhou et al. 2021), the imperviousness of the catchment surface and its spatial distribution (Gabellani et al. 2007; Paschalis et al. 2014; Pechlivanidis et al. 2017).

The impact of temporal characteristics of rainfall on outflow response has received less attention compared to spatial characteristics (Li et al. 2020). Aronica et al. (2005) investigated the influence of temporal resolution on the response of an urban catchment and concluded that rainfall data with low temporal resolution inevitably leads to an underestimation of the peak flow. Furthermore, the findings of several studies demonstrate that refining the temporal resolution leads to improved accuracy in simulating floods (Bruni et al. 2015; Chow et al. 2021; Hou et al. 2020; Huang et al. 2019; Li et al. 2022). In a similar study, Lyu et al. (2018), in addition to the aforementioned result, reported that the peak flow in comparison with the runoff volume is more sensitive to the temporal resolution of input rainfall data. As a result, there is still a need for further research to fully comprehend the influence of rainfall spatiotemporal variabilities on catchment response to either confirm or refuse the existing findings.

In this study, our aim is to comprehensively assess the effects of rainfall spatiotemporal variabilities on catchment response using a physically-based, fully distributed rainfall-runoff model, along with two rainfall generation models. We examined almost any factor that comes to mind when considering rainfall variabilities such as the location of the storm center, spatiotemporal resolutions of rainfall, and correlation length of rainfall fields in both space and time. The innovative aspect of this research lies within: 1- Developing two brand new simple rainfall generation models to address the research questions. 2- Simultaneously investigating the effect of rainfall resolution and rainfall correlation length in both time and space on catchment response. The main research questions were: (1) What would be the impact of storm

center location on catchment response? (2) How does the catchment respond to rainfall with different levels of spatial and temporal resolutions? (3) What would be the impact of rainfall correlation in time and space on catchment response?

2 Study Area and Data

2.1 Study Area

The study was focused on the Walnut Gulch Experimental Watershed (WGEW), a well-equipped catchment covering an area of 150 km^2 in Southeastern Arizona, USA (see Fig. 1). The climate of the region is classified as semi-arid, with mean annual temperature of 17.7 °C and mean annual precipitation of 350 mm. The precipitation regime is dominated by the North American Monsoon during July, August, and September. Elevation above mean sea level of the watershed ranges from 1250 to 1585 m.

The runoff characteristics of the WGEW are similar to those of many other semi-arid regions in the world, where the channels remain dry for most of the year (Stone et al. 2008). The streamflow regime is intermittent, lacking a base flow component, and the hydrographs exhibit a "flashy" nature primarily due to intense rainfall inputs. Consequently, the flood peak arrives rapidly with a steep rising limb in the flow hydrograph (Keppel and Renard 1962).

2.2 Rainfall and Runoff Data

The original rainfall and runoff measurement instruments on the WGEW were installed in 1950s. Currently, rainfall and runoff data in the catchment are collected via 97 operational tipping bucket rain-gauges and 16 hydrometric stations. The spatial distribution of these stations is shown in Fig. 1. Stream flows are monitored with one-minute temporal resolution, while precipitation is observed with variable temporal resolutions. In this research, data from 88 rain-gauges (See Table 5 in the Appendix A) with a considerable record length are used to parameterize the proposed stochastic rainfall generation model. Hydrometric station #7, documented in Table 6 in the Appendix A and illustrated in Fig. 1, drains a sub-catchment with a drainage area of 13.4 km^2. Considering hydrometric station #7 as the calibration point, this small sub-catchment, along with the data from 11 rain-gauges with symbol * in Table 5 in the Appendix A, is used in the actual calibration and verification phase of the employed rainfall-runoff model, MIKE-SHE (See appendix B for more details on the calibration and verification phase).

3 Methodology

3.1 Hydrologic Model

As the flow of water over the land phase of the hydrologic cycle is considered to be a distributed process, the estimates of flow rate and water level at important location(s) within the catchment can be obtained via a distributed flow routing model. With no exception, these types of models are based on partial differential equations (i.e., the

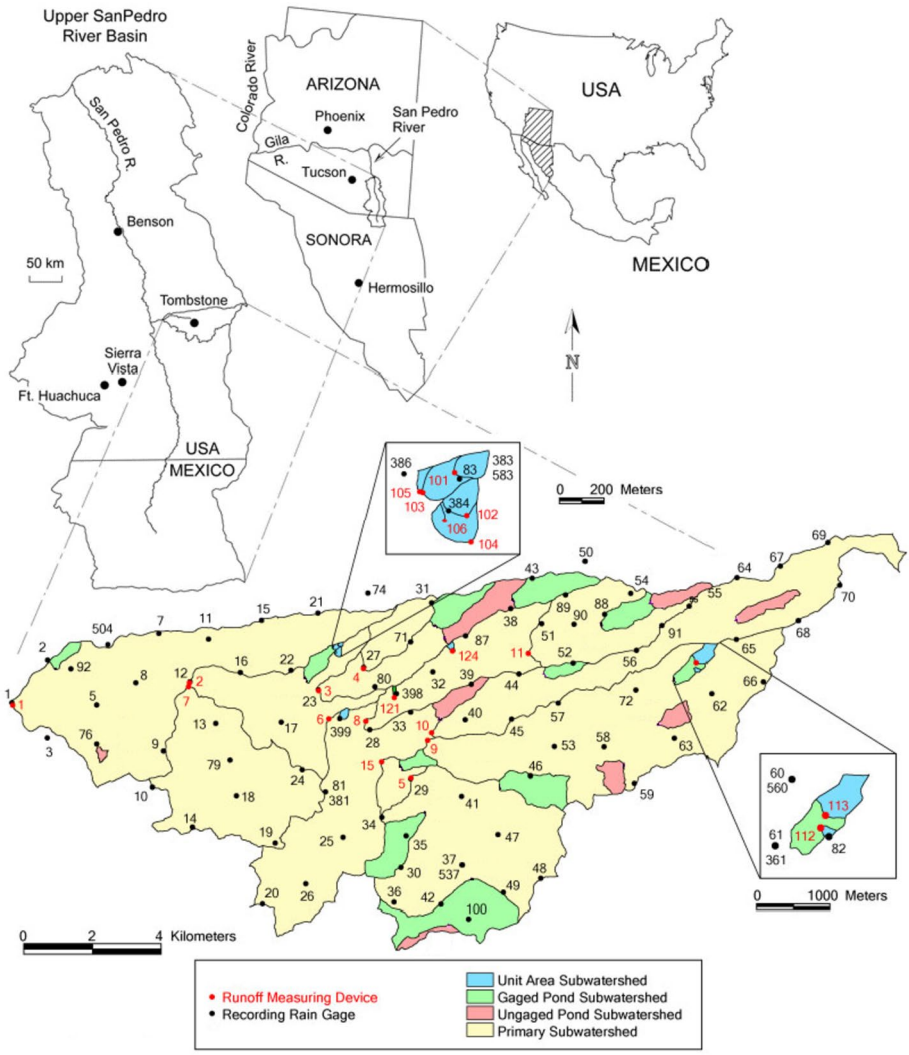

Fig. 1 Geographical location of Walnut Gulch Experimental Watershed and Spatial distribution of the rain-gauges and hydrometric stations

Saint–Venant equations for one-dimensional flow) that allow the flow rate and water level to be computed as functions of space and time (Chow et al. 1988). The nature of hydrologic numerical experiments calls for rainfall-runoff models which can accommodate both spatial and temporal variabilities of rainfall into account. As such, we used a physically-based, deterministic, and fully distributed hydrologic model called MIKE-SHE. MIKE-SHE is able to simulate all of the major hydrologic processes, including evapotranspiration, infiltration, overland flow, unsaturated flow, groundwater flow, and channel flow, as well as their interactions (Abbott et al. 1986). Depending on the goals of the modeling, the availability of field data, and the modeler's objectives, each of the cited processes can be represented at different levels of spatial distribution and complexity

(Butts et al. 2004). As an example, the precipitation input can be incorporated by assuming it to be uniform, station-based or fully distributed (grid-based).

The hydrologic processes simulated in this study were: overland flow, channel flow, and infiltration which were all triggered by a fully distributed precipitation input in all numerical experiments. As for infiltration, we utilized the Green-Ampt infiltration equation and its validity to convert raw rainfall to excess rainfall hyetograph was ensured via incorporation and independent verification of a rainfall temporal pattern (results are not included). We employed the two dimensional diffusive wave approximation of the Saint–Venant equations to route the overland flow process, and the major contribution to channel flow was assumed to be due to Hortonian overland flow [DHI (2014b), V.2 p.267]. For routing the upstream inflow hydrograph and the distributed lateral inflow caused by overland flow in the river corridor toward the mouth of the watershed, the fully dynamic version of MIKE-11 with suppression of convective term was utilized [DHI (2014a), p.457]. A Conventional finite difference method and the six-point Abbott-Ionescu scheme were respectively used to convert diffusion wave into algebraic equations for each spatial pixel in the catchment and to route the fully dynamic wave Saint–Venant equations in the river corridor[DHI (2014a), p.461]. The input parameters were considered to be precipitation, topography, Green-Ampt model infiltration parameters (i.e., saturated hydraulic conductivity, soil suction at wetting front, porosity, initial water content), overland and channel flow Manning roughness coefficients. All the data sources such as digital elevation model, channel network, ARC-GIS data layers, etc. used in the current study are available at https://www.tucson.ars.ag.gov/dap/.

3.2 Rainfall Generation Models

Rainfall generation models are typically categorized into various types based on their intended purpose. In this study, we pursued two primary objectives: first, to examine how the spatial location of the storm center influences the characteristics of the outflow hydrograph in the catchment, and second, to assess the impact of spatiotemporal variabilities of rainfall on these characteristics. To achieve these objectives, two straightforward rainfall generation models were developed and described in detail below.

3.2.1 Deterministic Rainfall Generation Model

One of the main objectives of this study is to examine how the spatial location of the storm center affects the outflow hydrograph of the catchment. To achieve this, it is imperative to generate events that share the same spatiotemporal pattern and volume, but with a significant change in the storm center location. For this purpose, we employed the bivariate normal distribution function as a mechanism to generate rainfall with the same spatial pattern and volume. The function ordinate of the mentioned distribution can be stated as follows:

$$f(x,y) = \frac{1}{2\pi\sigma_x\sigma_y\sqrt{1-\rho^2}} \exp\left\{ -\frac{\left[\frac{(x-\mu_x)^2}{\sigma_x^2} + \frac{(y-\mu_y)^2}{\sigma_y^2} - \frac{2\rho(x-\mu_x)(y-\mu_y)}{\sigma_x\sigma_y}\right]}{2(1-\rho^2)} \right\} \quad (1)$$

Once again, it should be noted that in this study, this relationship was used only as a function of x and y coordinates to generate rainfall spatial patterns of a specified coverage

and duration. μ_x and μ_y are the parameters that determine the location of the function maxima in x and y axes, respectively. σ_x and σ_y control the degree of sharpness or flatness of the peak. In this study, ρ, which dictates the degree of symmetry of the field, was assumed to be 0 in order to create symmetry in all directions in the generated spatial pattern. Needless to say, the pixel value for a particular x and y coordinates is considered to be the cumulative rainfall in that pixel. One of the features of this function is that the volume under the spatial pattern equals 1, meaning the function can be multiplied by any arbitrary number (V) to produce cumulative rainfall of a predefined volume. Assuming a triangular rainfall temporal pattern, we utilized the rainfall dimensionless temporal pattern documented in Fig. 2 to disaggregate the pixel value into a time-wise variation. As such, the duration of rainfall in all pixels is the same, but their total depth could be different.

3.2.2 Stochastic Rainfall Generation Model

This research aims to examine how the variability of rainfall in space and time affects the catchment outflow hydrograph. To this end, it is important to generate events with similar spatiotemporal correlation and volume. We employed the multivariate normal distribution function to generate rainfall events that share the same spatiotemporal structure and volume. The subsequent sections will provide a theoretical background and a detailed description of the rainfall generation model.

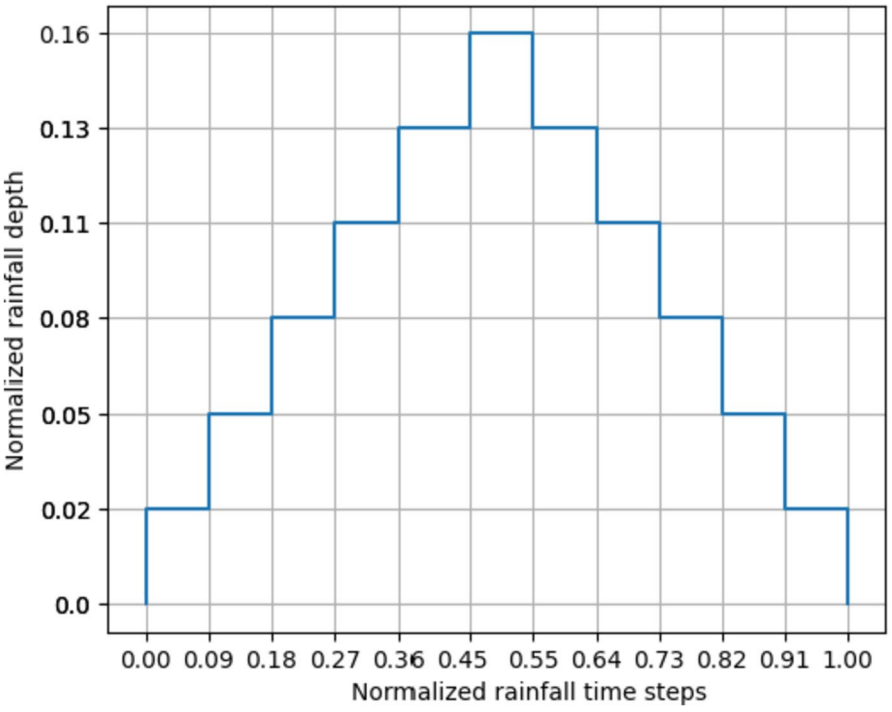

Fig. 2 The rainfall dimensionless temporal pattern used to convert cumulative rainfall to excess rainfall hyetograph

According to Bras and Rodríguez-Iturbe (1976), rainfall intensity as a function of space and time in a typical event can be defined as follows:

$$I(x, y, t) = I_{\mu}(x, y, t) + W(x, y, t) \tag{2}$$

where $I(x, y, t)$ is the rainfall intensity at a point (x, y) and at time t in the catchment, $I_{\mu}(x, y, t)$ is the mean deterministic component of rainfall intensity and $W(x, y, t)$ is the stochastic noisy residual with a zero mean and variance σ_w^2. It is generally accepted that the mean temporal rainfall pattern of the same type in a specific region can be represented in dimensionless form, as documented elsewhere (Eagleson 1970; Pilgrim and Cordery 1975). Therefore, one can compute $I_{\mu}(x, y, t)$ using rainfall data of any arbitrary gauged catchment. In this study, $I_{\mu}(x, y, t)$ was considered to be independent of space and only a function of time. In this regard, Eq. (2) can be rewritten as:

$$I(x, y, t) = I_{\mu}(t) + W(x, y, t) \tag{3}$$

Now, by computing $I_{\mu}(t)$ using historical rainfall data in a gauged catchment, it will be possible to generate a random event for the catchment by modeling $W(x, y, t)$ stochastically, as it is discussed in the next paragraph.

Assuming $W(x, y, t)$ to be a random process distributed in space and time, implies that at every point in space and at an instant in time, there is a random variable in the catchment. Suppose that the catchment can be spatially divided into m number of evenly distributed pixels with predefined dimensions and the event consists of n number of time-steps with predefined length. Therefore, there will be $N = m \times n$ random variables. Assuming the probability density function of these random variables (X_i;$i = 1, 2, 3, \ldots, N$) to be normal, their joint distribution function will be a multivariate normal distribution:

$$f_X(x_1, x_2, x_3, \ldots, x_N) = \frac{exp\left[-\frac{1}{2}(\mathbf{x} - \boldsymbol{\mu})^T \sum^{-1} (\mathbf{x} - \boldsymbol{\mu})\right]}{\sqrt{(2\pi)^N |\sum|}} \tag{4}$$

where $\boldsymbol{x}$ is a real N-dimensional column vector, $\boldsymbol{\mu}$ is the mean vector and $\sum$ is an $N \times N$ variance–covariance matrix which are defined as follow:

$$\boldsymbol{\mu} = \left\{E\left[X_1\right], E\left[X_2\right], E\left[X_3\right], \ldots, E\left[X_N\right]\right\} \tag{5}$$

$$\sum = \left[COV\left(X_i, X_j\right); 1 \le i, j \le N\right] \tag{6}$$

In which:

$$COV\left(X_i, X_j\right) = \sigma_i \sigma_j \rho(X_i, X_j) \tag{7}$$

In Eqs. (4), (5), (6) and (7) $E[]$ is the expectation operator, $COV\left(X_i, X_j\right)$ is the covariance of X_i and X_j, σ_i is the standard deviation of X_i, and $\rho(X_i, X_j)$ is the correlation function between X_i and X_j. As a result, after specifying the parameters of the distribution function [i.e., the mean vector and the variance–covariance matrix, $N(\mu, \sigma, \alpha)$], it is feasible to sample the field of $W(x, y, t)$ stochastically, and generate various realizations of a typical random field with a specified spatial and temporal correlation.

As $W(x, y, t)$ is a zero mean random field, the members of the mean vectors are all zero. Specifying the entries of the covariance matrix, according to Eq. (7), requires knowing the

standard deviation of each random variable and the correlation between the random variables X_i and X_j. We extensively utilized rainfall data of WGEW in time and space to establish parameters of the variance–covariance function. Then, the separation distance and lag between pixels were used to obtain entries of the variance–covariance matrix.

To find the correlation between the random variables X_i and X_j at two different instances, the following spatiotemporal correlation structure was employed (Porcu et al. 2020):

$$\rho(\Delta h, \Delta t) = exp\,(-\frac{\Delta h}{\alpha}) \times exp\,(-\frac{\Delta t}{\beta}) \tag{8}$$

where Δh and Δt are the separation distance and time lag between X_i and X_j, respectively. α and β are the autocorrelation lengths in space and time, controlling the spatial and temporal variations of the attribute under consideration over the study area. Once again, observed rainfall data of WGEW were used to extract correlation parameters in time and space and delineate the spatiotemporal experimental and subsequently theoretical variograms. Needless to say, we assumed that the random field is stationary (i.e., mean and variance are independent of space and are constant) and isotropic (i.e., the theoretical variogram's parameters would not change with direction).

3.3 Calibration and Verification of MIKE-SHE Model for a Sub-Watershed of Walnut Gulch Catchment

The main focus of this study was to utilize the WGEW for numerical experiments and to examine how the spatiotemporal variabilities of rainfall affect catchment response. The purpose of conducting actual model calibration and subsequent verification was not to calibrate the model for practical applications, but rather to ensure that we as the potential user understand the underlying logic of the simulation program. Appendix B provides a brief description of the calibration and independent verification of the MIKE-SHE model.

3.4 Detail of Numerical Experiments Design

In this subsection, a rational will be provided on how the data for each research question was generated. For this purpose, synthetic rainfall events were generated using the two rainfall generation models introduced earlier. In all cases, the catchment area was divided into 591 pixels of size 500 m × 500 m, and the generated hyetograph for each pixel was used in the modeling. Additionally, in all the experiments, the rainfall-runoff process has been modeled in the entire Walnut Gulch catchment with a basin area of 150 km^2, using a reasonable but not calibrated set of parameters. We executed the rainfall-runoff model in a forward manner with a synthetic forcing function (i.e., rainfall input), hypothetical soil hydraulic properties compatible with watershed characteristics, watershed topographic pattern, etc. (See Table 1). It should be noted that all these values were chosen reasonably, taking into account the real physical characteristics of the catchment.

Table 1 Numerical values of input parameters in MIKE-SHE

Parameter name	Parameter value	Parameter dimension	Spatially uniform/ distributed	Recommended by
Overland flow Manning's M	30	$m^{1/3}/s$	Uniform	[DHI (2014b), V. 1]
Channel flow Manning's M	30	$m^{1/3}/s$	Uniform	[DHI (2014b), V. 1]
Soil suction at wetting front-Sandy loam	-0.11	m	Uniform	(Chow et al. 1988)
Saturated hydraulic conductivity- Sandy loam	3.03×10^{-6}	m/s	Uniform	(Chow et al. 1988)
Saturation moisture content- Sandy loam	0.45	-	Uniform	(Chow et al. 1988)
Moisture content at field capacity- Sandy loam	0.14	-	Uniform	(Chow et al. 1988)
Moisture content at wilting point- Sandy loam	0.05	-	Uniform	(Chow et al. 1988)

The Manning's M is the inverse of the more conventional Manning's n

3.4.1 Test Case #1

The main aim of test case #1 was to examine how the location of the storm center influences the characteristics of the outflow hydrograph. For this purpose, ten synthetic rainfall events were generated using the deterministic rainfall generation model. These events shared the same spatial pattern, nearly the same volume, but different storm center locations. In this particular case, the watershed was assumed to be impermeable, meaning that the original rainfall hyetograph was excess rainfall. To determine the location of the storm center relative to the outlet of the catchment, we employed the index I_{pcp}, introduced by Smith et al. (2004), as a numerical measure. This index is defined as follows:

$$I_{pcp} = \frac{C_{pcp}}{C_{basin}} \tag{9}$$

In which:

$$C_{pcp} = \frac{\sum_{i=1}^{N_p} P_i A_i L_i}{\sum_{i=1}^{N_p} P_i A_i} \tag{10}$$

$$C_{basin} = \frac{\sum_{i=1}^{N_p} A_i L_i}{\sum_{i=1}^{N_p} A_i} \tag{11}$$

where, N_p is the number of input rainfall pixels (in this case 591), P_i is the amount of event cumulative rainfall depth for pixel i, A_i is the area covered by pixel i (which is the same for all pixels), L_i is the hydraulic distance between pixel i and the catchment outlet, calculated via ArcMap.

The closer I_{pcp} is to 1, the closer the storm center is to the catchment center. Values greater than 1 indicate that the storm center is closer to the upstream, while values less than 1 imply that the storm center is closer to the downstream. All 10 events were modeled using MIKE-SHE and the values of time to peak and peak magnitude were compared, considering I_{pcp} of events and excluding runoff volume due to its invariance property for all events.

3.4.2 Test Case #2

The purpose of designing test case #2 was to investigate the effect of rainfall spatiotemporal variabilities (i.e., rainfall spatial and temporal measurement scales and correlation length in time and space) on the characteristics of outflow hydrograph. Rainfall spatial and temporal measurement scales represent themselves in resampling the spatial and/or temporal resolutions.

To achieve this objective, we generated three sets of rainfall events using the stochastic rainfall generation model, with each set consisting of 25 synthetically generated realizations, all with similar rainfall volume and spatiotemporal resolution. However, the sets differed in their spatiotemporal correlation structures. The parametric characteristics for each set of events are summarized in Table 2.

We used events from series #1 and #2 to investigate the effect of rainfall spatial resolution, for two correlation lengths in space, on catchment response. To this end, 1 km × 1 km, 1.5 km × 1.5 km, 2 km × 2 km, 3 km × 3 km, 6 km × 6 km and spatially uniform versions

Table 2 Characteristics for each series of generated events

	Event series number		
	1	2	3
Number of events	25	25	25
Reference spatial resolution	0.5 km × 0.5 km	0.5 km × 0.5 km	0.5 km × 0.5 km
Reference temporal resolution	10 min	10 min	10 min
Correlation length in space	15.6 km	5.2 km	15.6 km
Correlation length in time	18.3 min	18.3 min	55 min
Resampled spatial resolution	1 km × 1 km 1.5 km × 1.5 km 2 km × 2 km 3 km × 3 km 6 km × 6 km Uniform	1 km × 1 km 1.5 km × 1.5 km 2 km × 2 km 3 km × 3 km 6 km × 6 km Uniform	-
Resampled temporal resolution	20 min 30 min 40 min	-	20 min 30 min 40 min

of each event, were obtained by spatial aggregation of benchmark event (i.e., 500 m × 500 m spatial resolution, temporal resolution remains at 10-min). Finally, by considering the simulated outflow hydrographs for 500 m × 500 m scenario as the reference hydrographs, we compared the characteristics of outflow hydrographs of the 6 remaining versions of each event for series #1 and #2 with the reference hydrographs. In order to validate the difference in the spatial correlation of the two series, Moran's I index was employed, which is defined as follows (Zhang and Han 2017):

$$I = \frac{N_P}{W_P} \frac{\sum_i \sum_j w_{ij}(P_i - \overline{P})(P_j - \overline{P})}{\sum_i (P_i - \overline{P})} \tag{12}$$

where N_p is the number of points or pixels (in this case 591), P_i is the cumulative depth of precipitation for pixel i, $\overline{P}$ is the average depth of precipitation over the catchment area and:

$$\begin{aligned} w_{ij} &= r_{ij}^{-1} \text{ for } i \neq j \\ w_{ij} &= 0 \text{ for } i = j \end{aligned} \tag{13}$$

$$W_p = \sum_i \sum_j w_{ij} \tag{14}$$

In which r_{ij} is the spatial distance between pixels i and j.

Similarly, we investigated the impact of rainfall temporal resolution on the characteristics of the outflow hydrograph using events from series #1 and #3. To do this, different versions of each event were created by temporally aggregating the benchmark event (which has a 10-min temporal resolution) into 20-min, 30-min, and 40-min versions. The spatial resolution remains constant at 500 m × 500 m. Consequently, we compared the characteristics of the outflow hydrographs for the three upscaled versions of each event from series #1 and #3 with the reference hydrographs. Considering the existing literature in mind, in the following section, the results of each experiment and their practical implications in operational hydrology, will be presented.

3.5 Measures of Accuracy

In this research, two measures of goodness, namely *NRMSE* (Normalized Root Mean Square Error) and Relative Error, were utilized to compare and evaluate various scenarios emerging from the experimental design. They are defined as follows:

$$NRMSE = \frac{\sqrt{\frac{\sum_{i=1}^{E}(y_i^s - y_i^r)^2}{E}}}{\overline{y}} \tag{15}$$

$$Relative\ Error = \frac{y_i^s - y_i^r}{\overline{y}} \tag{16}$$

where y_i^r is the reference value for event i, y_i^s is the simulated value for event i, E is the number of events, $\overline{y}$ is the average of the reference values (the values could be peak magnitude, time to peak, and runoff volume).

4 Results and Discussion

4.1 Test Case #1

Figure 3a and b display the spatial pattern of cumulative rainfall events for two extreme scenarios, namely events #1 and #10. It is evident from these figures that the only difference among the generated patterns lies within the location of the storm center. It is hypothesized that despite having the same spatiotemporal pattern and rainfall volume, these events would result in completely different outflow hydrographs due to variations in the storm center location.

Figure 3c, d illustrate the peak magnitude and time to peak as a function of I_{pcp} for various events. As expected, an increase in I_{pcp}, which corresponds to an increase in the distance between the storm center and the outlet, leads to substantial variations in both peak magnitude and time to peak, following a clearly defined trend. Specifically, as the storm center moves away from the catchment outlet, the outflow hydrograph attenuates, resulting in a decrease in peak magnitude. Additionally, an increase in I_{pcp} leads to a longer travel time for the flood peak, resulting in an increase in time to peak (Smith et al. 2004). Regarding the time to peak, Chen et al. (2023) also achieved similar results. However, in terms of peak magnitude, they reported a different behavior (i.e., a double peak hydrograph for the case with the storm center locating in the downstream), possibly due to variations in topography and the asymmetric nature of the events being studied. Michelon et al. (2021) similarly indicated that the distance between the rainfall center and the outlet can have a significant impact on the hydrologic response.

Figure 3e further demonstrates how the change in storm center location affects the outflow response in two ways: attenuation and translation of peak discharge. This is evident in events #1 and #10, which represent the farthest and nearest scenarios to the catchment outlet, respectively. Event #1 exhibits a considerable amount of attenuation and an increase in lag time of the hydrograph. These observations have practical implications for defining worst-case scenarios in designing hydraulic structures and determining the optimal spatial location for flood-mitigating structures, such as check dams.

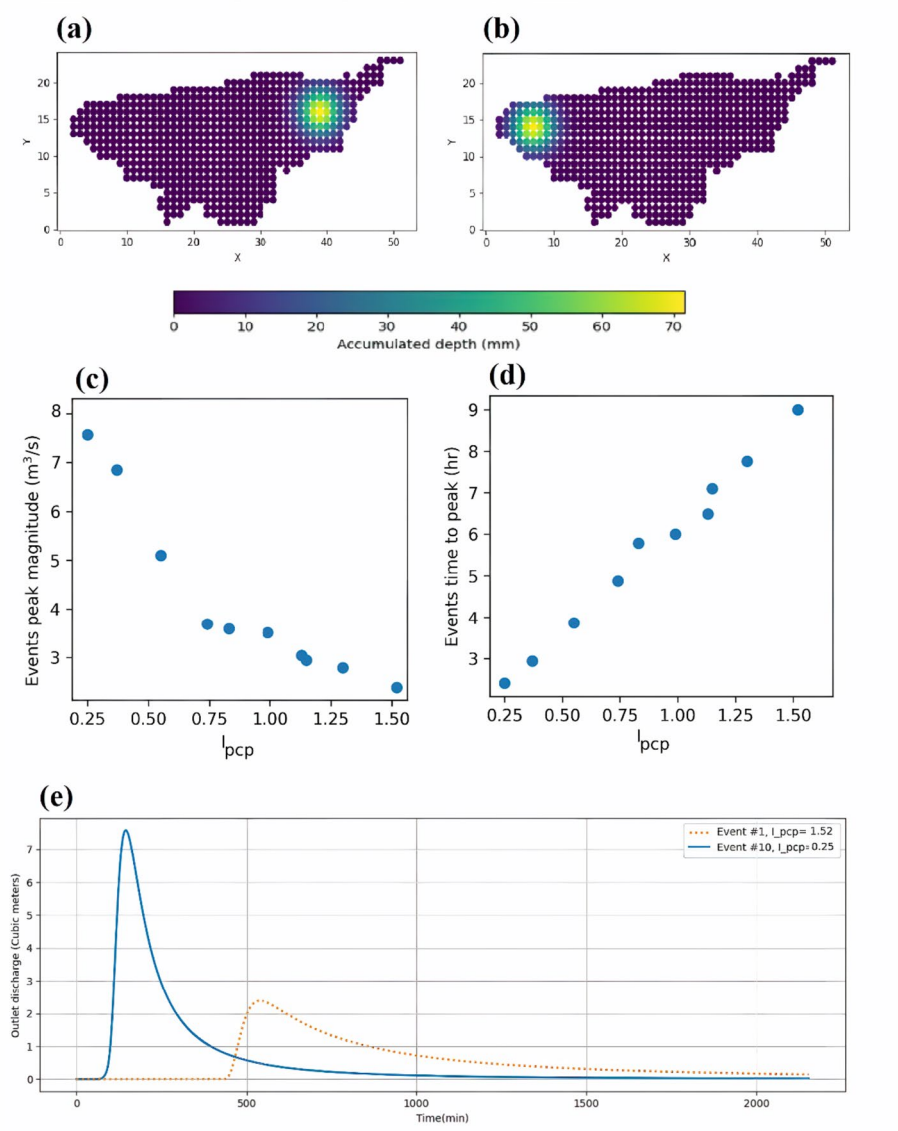

Fig. 3 **a**, **b** Accumulated rainfall spatial pattern for two extreme scenarios–Events #1 and #10, variation of peak magnitude and time to peak against I_{pcp} **c** Flood peak magnitude, **d** time to peak, **e** Outflow hydrographs for two extreme scenarios–Events #1 and #10

4.2 Test Case #2

Test case #2 is divided into two parts. Firstly, it examines the influence of rainfall spatial variability (i.e., resolution and correlation in space) on catchment response. This involves modeling rainfall observations at a 500 m grid spacing and 10-min intervals, as well as the resampled version at coarser resolutions (i.e., series #1 and #2). The resulting runoff hydrographs are then assessed.

Secondly, the test case evaluates the impact of rainfall temporal variability (i.e., resolution and correlation in time) on catchment response. This is done by modeling rainfall observations at a 500 m grid spacing and 10-min intervals, and the resampled versions at lower temporal resolutions (i.e., series #1 and #3). The subsequent runoff hydrographs are then critically evaluated.

4.2.1 Impact of Rainfall Spatial Variability

Figures 4a–f, g–l, m–r indicate the variation of flood peak magnitude, time to peak, and runoff volume, respectively, obtained from upscaled events in space compared to the reference spatial resolution for both series #1 and #2, considering two correlation lengths in space. For a fixed correlation length in space, increasing the spatial measurement scale (resampling in space) initially has minimal impact on the peak magnitude, time to peak, and runoff volume. However, at higher resampling resolutions, particularly with uniform sampling, there is a considerable departure from the benchmark solutions, leading to underestimation of flood peak magnitude (Fig. 4a–f) and runoff volume (Fig. 4m–r), and overestimation of time to peak (Fig. 4g–l). The underestimation of peak magnitude has been observed in previous studies (Arnaud et al. 2011; Kim and Kim 2020; Krajewski et al. 1991; Li et al. 2020; Lobligeois et al. 2014; Meselhe et al. 2009) and is attributed to the smoothing of rainfall patterns for upscaled events, resulting in the replacement of high-intensity pixels with lower ones. The literature lacks a clear consensus on the effect of spatial resampling on the time to peak. For instance, Cristiano et al. (2019) obtained similar findings to the current research, while Bruni et al. (2015) discovered that spatially upscaled events can lead to either an increase or decrease in the time to peak, depending on specific event characteristics. Therefore, it remains challenging to make a definitive statement regarding this Issue. Furthermore, resampling in space leads to underestimation of runoff volume, potentially due to increased infiltration as rainfall intensity decreases below the potential infiltration rate (Sapriza-Azuri et al. 2015).

The impact of spatial density of the monitoring network (i.e., spatial measurement scale) on hydrograph characteristics is influenced by the spatial correlation of rainfall. Higher spatial correlation leads to a lower impact of spatial measurement scale on the peak magnitude (Bell and Moore 2000). This has implications for rain-gauge network design, particularly when considering spatiotemporal variations to refine flood hydrograph characteristics (Attar et al. 2020; Shahidi and Abedini 2018; Soroush and Abedini 2019). Furthermore, a higher spatial correlation diminishes the influence of spatial density on the time to peak. However, this effect is not as pronounced as the impact on the magnitude of the peak. This implies that rainfall spatial information has less impact on overestimation of time to peak compared to underestimation of peak magnitude. Assigning a uniform spatial distribution of rainfall to flood warning systems, while converting rainfall into runoff, appears to be misleading and could potentially lead to severe property damage and human casualties (Lin et al. 2022).

The results can be further explained by utilizing an index known as *NRMSE*. A lower value of this index indicates a closer match between the simulated values (obtained from upscaled events) and the benchmark values. Table 3 displays the *NRMSE* values for peak magnitude, time to peak, and runoff volume for both low and high spatially correlated events. It is evident that resampling in space results in an increase in *NRMSE*. The rate of increase for peak magnitude is particularly notable compared to other hydrograph

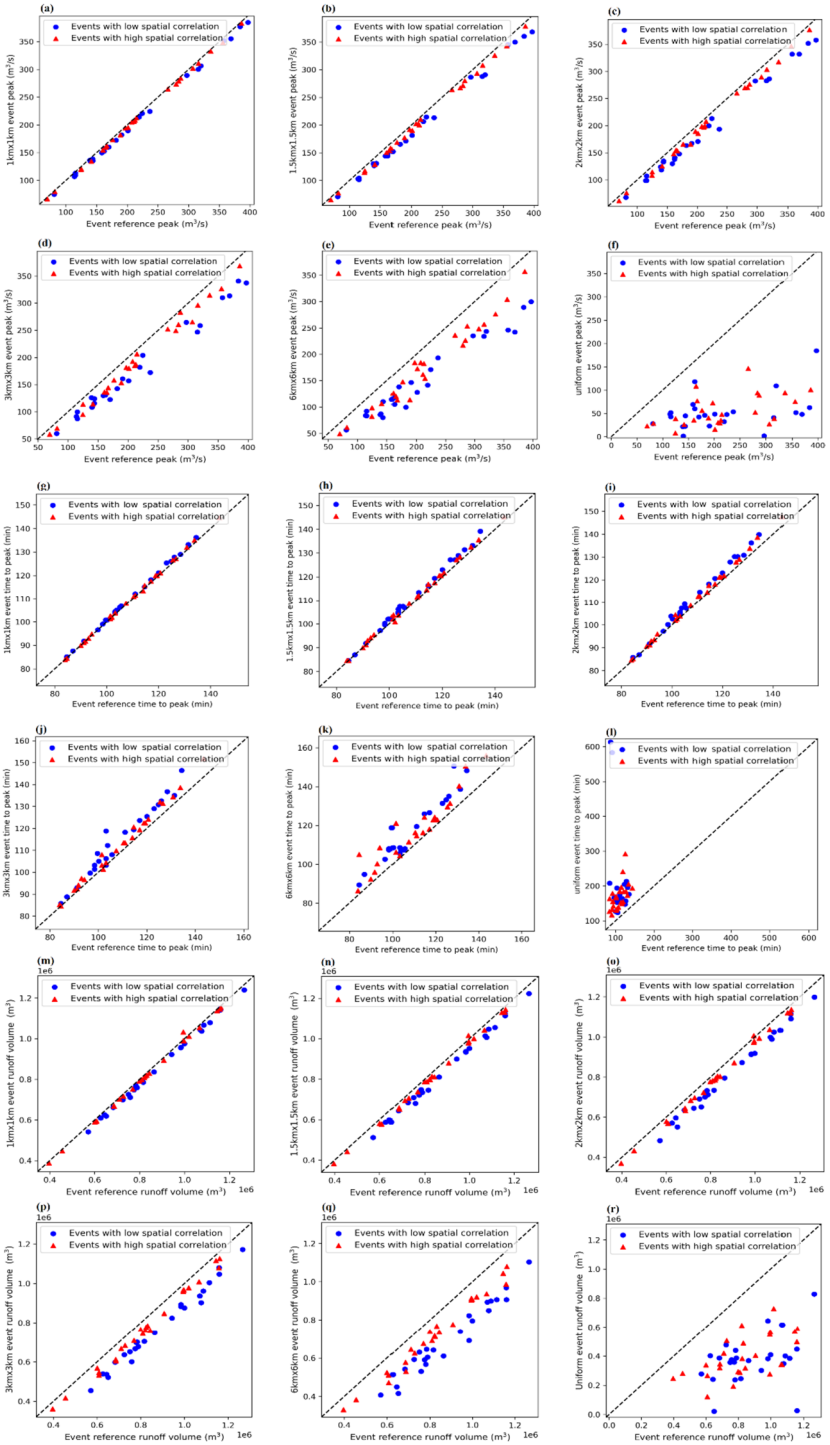

Fig. 4 Effect of spatial upscaling on **a-f** peak magnitude **g-l** time to peak **m-r** runoff volume for events with both high (events series #1) and low (events series #2) spatial correlation

Table 3 *NRMSE* values for peak magnitude, time to peak and runoff volume in events with both high (events series #1) and low (events series #2) spatial correlation

	Spatial resolutions					
	1 km × 1 km	1.5 km × 1.5 km	2 km × 2 km	3 km × 3 km	6 km × 6 km	Uniform
Peak magnitude—Low correlation in space	0.04	0.08	0.11	0.18	0.31	0.85
Peak magnitude—High correlation in space	0.02	0.04	0.05	0.1	0.2	0.81
Time to peak—Low correlation in space	0.05	0.05	0.05	0.08	0.1	1.43
Time to peak—High correlation in space	0	0.01	0.01	0.03	0.08	0.62
Runoff volume—Low correlation in space	0.03	0.05	0.08	0.12	0.21	0.61
Runoff volume—High correlation in space	0.01	0.02	0.03	0.06	0.12	0.55

characteristics, consistent with the earlier explanations. In general, spatial aggregation of events leads to a decrease in peak magnitude, an increase in time to peak, and a decrease in runoff volume. This is illustrated in Fig. 5a, which showcases a hydrograph for a typical event alongside its corresponding resampled event in space. It is crucial to note that underestimation of peak magnitude and runoff volume, as well as overestimation of time to peak, can all contribute to greater flood damage. Therefore, the density of the rainfall monitoring network plays a significant role in mitigating losses associated with floods.

A more detailed examination of the information presented in Table 3 suggests that events with higher spatial correlation exhibit lower *NRMSE* values compared to events with lower spatial correlation. In other words, the impact of monitoring network density on the outlet hydrograph is closely tied to the spatial correlation of the event. Consequently, the magnitude of this impact is expected to be influenced by the climatic conditions and rainfall regime of the region, which determine the characteristics of the rainfall events. Therefore, the required density of the monitoring network to accurately estimate the catchment outlet hydrograph will vary depending on the catchment and its specific climatic conditions.

To further support the findings of this study, Figs. 6a–f, g–l demonstrate the variation in relative error of peak values and time to peaks against variation in the coefficient of variation (CV) and Moran's I, respectively. In these figures, the ordinate of relative error for both peak and time to peak values is demonstrated with different colors. Zhang and Han (2017) attempted to classify rainfall spatial variability based on simultaneous variations in

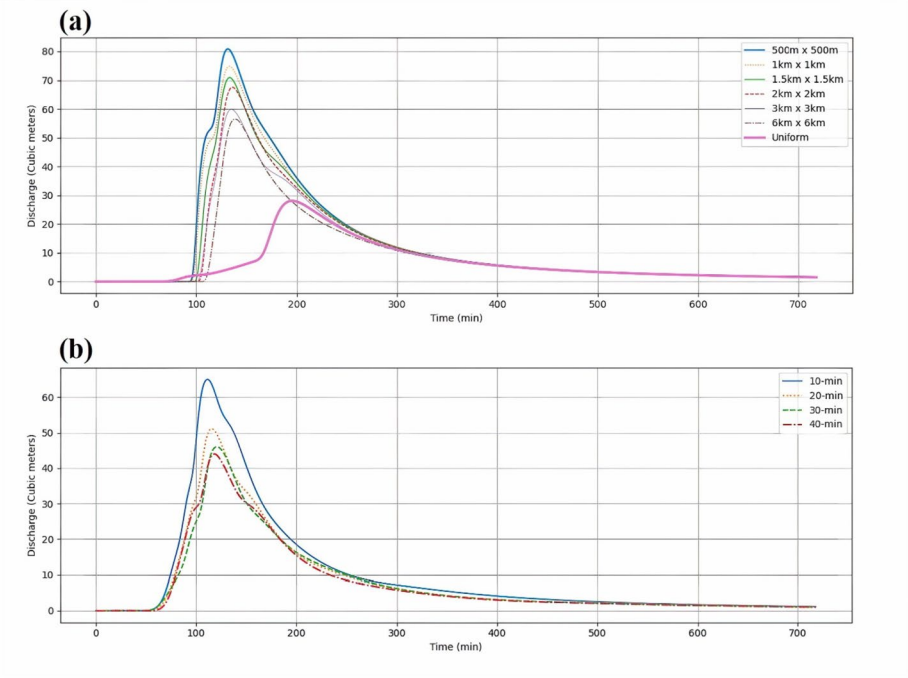

Fig. 5 **a** WGEW's outlet hydrograph for a typical reference event. Spatial resolution: 500 m × 500 m, Temporal resolution: 10-min along with other resampled hydrographs with various spatial resolution (1 km × 1 km, 1.5 km × 1.5 km, 2 km × 2 km, 3 km × 3 km, 6 km × 6 km and spatially uniform) **b** WGEW's outlet hydrograph for a typical reference event. Spatial resolution: 500 m × 500 m, Temporal resolution: 10-min along with other resampled hydrographs with various temporal resolution (20-min, 30-min and 40-min)

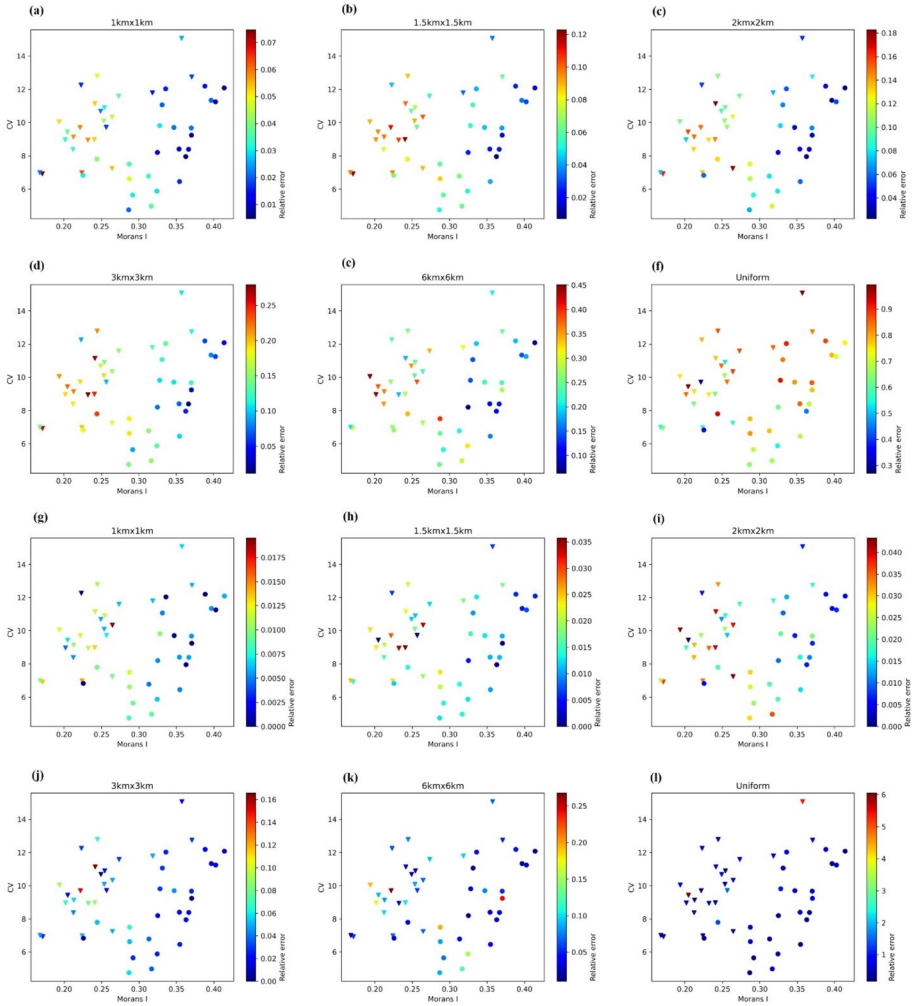

Fig. 6 Variation of relative error in **a-f** peak magnitude and **g-l** time to peak as a function of Moran's I index and coefficient of variation

indices such as the CV and Moran's I. According to their classification, a complex event is characterized by low values of Moran's I and high values of CV, while a simple event has high values of Moran's I and low values of CV. Other alternatives are considered medium events. It is important to note that the color bar will vary depending on the resampling scale. As observed, for all spatial resolutions, events with lower values of Moran's I and either lower or higher values of CV exhibit greater relative error in both peak magnitude and time to peak. This suggests that the relative error is more sensitive to changes in the Moran's I index compared to the CV. This discrepancy can be attributed to the fact that the CV, unlike the Moran's I index, is not closely linked to the spatial pattern of precipitation.

4.2.2 Impact of Rainfall Temporal Variability

Figure 7a–c, d–f, g–i show the variation in flood peak magnitude, time to peak, and runoff volume obtained from resampled events in time compared to the corresponding values at the reference temporal resolution for both series #1 and #3, considering two correlation lengths in time. The results of the numerical experiments indicate that peak magnitude and runoff volume are lower, while time to peak is higher, in the temporally upscaled events compared to the reference hydrographs generated using 10-min events. This can be argued by the smoothing of the temporal pattern of rainfall in the upscaled events, resulting in a reduction in high-intensity hyetographs. This is depicted in Fig. 5b, which illustrates a hydrograph for a typical event and its corresponding resampled events in time. These findings are in line with earlier research studies (Aronica et al. 2005; Hou et al. 2020; Huang et al. 2019). Similar to the spatial upscaling, the coarser the temporal resolution is, the lower the peak magnitudes and the higher the time to peaks are, compared to the reference values. Similar behavior is observed elsewhere (Cristiano et al. 2019; Lyu et al. 2018; Ochoa-Rodriguez et al. 2015).

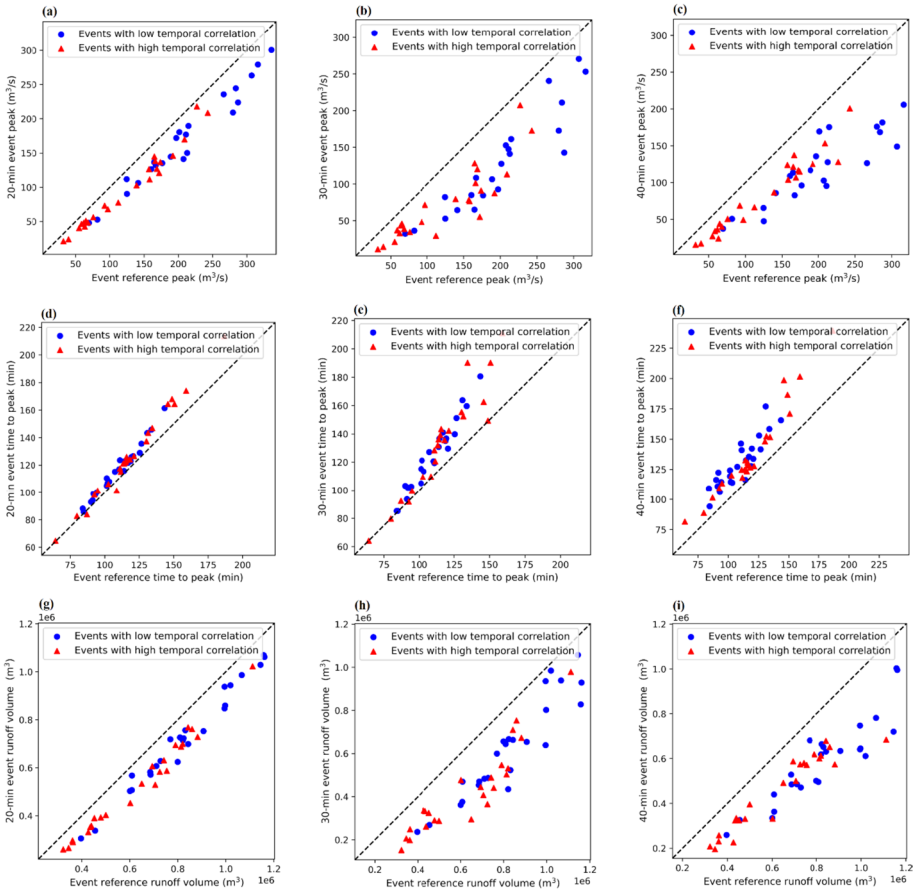

Fig. 7 Effect of temporal upscaling on **a-c** peak magnitude, **d-f** time to peak magnitude and **g-i** runoff volume for events with both low (events series #1) and high (events series #3) temporal correlation

Table 4 *NRMSE* error index for peak magnitude, time to peak and runoff volume in events with high temporal correlation (events series #3) and events with low temporal correlation (events series #1)

	Temporal resolutions		
	20 min	30 min	40 min
Peak magnitude—Low correlation in time	0.18	0.37	0.41
Peak magnitude—High correlation in time	0.23	0.48	0.36
Time to peak—Low correlation in time	0.07	0.15	0.2
Time to peak—High correlation in time	0.09	0.22	0.19
Runoff volume—Low correlation in time	0.12	0.26	0.3
Runoff volume—High correlation in time	0.17	0.34	0.29

It is important to note that the differences between the reference hydrographs and the hydrographs of events that have been upscaled temporally are more prominent than the differences between the reference hydrographs and the hydrographs of events that have been upscaled spatially. This suggests that temporal aggregation has a greater impact on hydrograph characteristics compared to spatial aggregation (Liu et al. 2021; Ochoa-Rodriguez et al. 2015).

Table 4 presents the *NRMSE* values for peak magnitude, time to peak, and runoff volume for low and high temporally correlated events. The *NRMSE* values for events with different levels of temporal correlation do not exhibit significant differences. However, it is important to note that reaching a definitive conclusion on this matter requires more extensive research, as there is a lack of similar studies in the existing research literature for comparative analysis.

5 Conclusions

This research intended to investigate the impact of storm center location, spatiotemporal variabilities, and correlation structure of rainfall in time and space on the catchment outflow response. For the first objective, 10 events with almost the same volume and temporal pattern but different storm center locations were generated using deterministic rainfall generation model, and the resulting hydrographs were compared. The findings showed that when the storm center was closer to the catchment outlet, the peak magnitude increased significantly while the time to peak decreased. This has implications for designing hydraulic structures and flood mitigation measures within a typical catchment.

For the second objective, the impact of rainfall spatial variability on catchment response was explored using two sets of events with different spatial correlation structures and almost the same volume and temporal correlation structure, generated by a stochastic rainfall generation model. The results showed that the spatial density of the monitoring network had a significant impact on the hydrological response of the catchment, particularly on the peak magnitude. The effect of spatial density was lower for events with higher spatial correlation.

Similarly, the impact of rainfall temporal variability on outlet discharge was investigated using two sets of events with different temporal correlation structures and almost the same volume and spatial correlation structure, generated by a stochastic rainfall generation model. The time step of the monitoring network had a considerable effect on the outflow hydrograph characteristics, with temporal resolution having a greater impact than spatial

resolution. This implies call for a more refined resolution in time compared to space. The results also indicate that the peak magnitude was the most sensitive component to temporal resolution, and the effect of temporal resolution was not significantly influenced by temporal correlation.

The results of this study have the potential to improve flood monitoring and warning systems, as well as optimize the design of rain gauge networks and drainage systems, specifically in urban catchments. This is achieved by highlighting the importance of having a rainfall measurement system that is both spatially and temporally dense. In this research, the density of the rainfall measurement system is assumed to be relatable to the spatial resolution of rainfall while one can generate rainfall events at irregular points in space (representing the irregular nature of rain gauges' distribution) using the developed rainfall-runoff model and carry out similar experiments to put the findings of this study on a sounder argument. In this regard, the main difference would be the fact that upscaling means averaging some piece of information whereas crossing gauges out of a network means losing information. However, one limitation is that the study used synthetic data, and further research is needed to verify the results using real-world catchment data and address other sources of uncertainty and interactions between spatiotemporal variability of soil hydraulic properties. In summary, this study highlights the importance of a dense rain-gauge network with a short monitoring time step to accurately capture the spatiotemporal correlation structure and pattern of rainfall for reliable estimation of the outflow hydrograph.

Supplementary Information The online version contains supplementary material available at https://doi.org/10.1007/s11269-023-03610-0.

Author Contributions All authors contributed to the study conception and design.

Data Availability Some or all data, models, or code that support the findings of this study are available from the corresponding author upon reasonable request.

Declarations

Consent for Publication During the preparation of this work the authors used ChatGPT in order to make the manuscript readable and easy to follow. After using this tool/service, the authors reviewed and edited the content as needed and take full responsibility for the content of the publication.

Competing Interests The authors have no relevant financial interests to disclose.

References

Abbott MB, Bathurst JC, Cunge J, O'Connell P, Rasmussen J (1986) An introduction to the European Hydrological System — Systeme Hydrologique Europeen, "SHE", 1: History and philosophy of a physically-based, distributed modelling system. J Hydrol 87(1–2):45–59. https://doi.org/10.1016/0022-1694(86)90114-9

Arnaud P, Lavabre J, Fouchier C, Diss S, Javelle P (2011) Sensitivity of hydrological models to uncertainty in rainfall input. Hydrol Sci J 56(3):397–410. https://doi.org/10.1080/02626667.2011.563742

Aronica G, Freni G, Oliveri E (2005) Uncertainty analysis of the influence of rainfall time resolution in the modelling of urban drainage systems. Hydrol Process 19(5):1055–1071. https://doi.org/10.1002/hyp.5645

Attar M, Abedini MJ, Akbari R (2020) Point versus block ordinary kriging in rain gauge network design using artificial bee colony optimization. Iran J Sci Technol Trans Civil Eng 45(3):1805–1817. https://doi.org/10.1007/s40996-020-00484-9

Bell VA, Moore RJ (2000) The sensitivity of catchment runoff models to rainfall data at different spatial scales. Hydrol Earth Syst Sci 4(4):653–667. https://doi.org/10.5194/hess-4-653-2000

Beven KJ (ed) (2012) Rainfall-runoff modeling: The primer. John Wiley and Sons, New York, pp 360

Beven KJ, Hornberger GM (1982) Assessing the effect of spatial pattern of precipitation in modeling stream flow hydrographs. J Am Water Resour Assoc 18(5):823–829. https://doi.org/10.1111/j.1752-1688.1982.tb00078.x

Blöschl G et al (2019) Twenty-three unsolved problems in hydrology (UPH)- A community perspective. Hydrol Sci J 64(11):1141–1158. https://doi.org/10.1080/02626667.2019.1620507

Bras RL, Rodríguez-Iturbe I (1976) Rainfall generation: A nonstationary time-varying multidimensional model. Water Resour Res 12(3):450–456. https://doi.org/10.1029/wr012i003p00450

Bruni G, Reinoso R, van de Giesen NC, Clemens FHLR, ten Veldhuis JAE (2015) On the sensitivity of urban hydrodynamic modelling to rainfall spatial and temporal resolution. Hydrol Earth Syst Sci 19(2):691–709. https://doi.org/10.5194/hess-19-691-2015

Butts MB, Payne JT, Kristensen M, Madsen H (2004) An evaluation of the impact of model structure on hydrological modelling uncertainty for streamflow simulation. J Hydrol 298(1–4):242–266. https://doi.org/10.1016/j.jhydrol.2004.03.042

Caracciolo D, Arnone E, Noto LV (2014) Influence of spatial precipitation sampling on hydrological response at the catchment scale. J Hydrol Eng 19(3):544–553. https://doi.org/10.1061/(asce)he.1943-5584.0000829

Carvalho RC, Woodroffe CD (2015) Rainfall variability in the Shoalhaven River catchment and its relation to climatic indices. Water Resour Manag 29(14):4963–4976. https://doi.org/10.1007/s11269-015-1098-4

Chen G, Hou J, Hu Y et al (2023) Simulated investigation on the impact of spatial–temporal variability of rainstorms on flash flood discharge process in small watershed. Water Resour Manag 37:995–1011. https://doi.org/10.1007/s11269-022-03398-5

Chow MF, Haris H, Leong XY (2021) The effect of temporal resolution of input rainfall data in hydrological modelling at urban catchment. AIP Conf Proc 2339:020074. https://doi.org/10.1063/5.0044479

Chow VT, Maidment DR, Mays LW (1988) Applied hydrology, 2nd edn. McGraw–Hill Book Co., New York, pp 572

Cristiano E, Veldhuis M, Wright DB, Smith JA, Giesen N (2019) The influence of rainfall and catchment critical scales on urban hydrological response sensitivity. Water Resour Res 55(4):3375–3390. https://doi.org/10.1029/2018wr024143

Danish Hydraulic Institute (DHI) (2014a) Modelling system for rivers and channels Reference Manual, Hørsholm, Denmark

Danish Hydraulic Institute (DHI) (2014b) MIKE-SHE User Manual, Vol. 1 & 2: User & Reference Guide, Hørsholm, Denmark

Eagleson PS (1970) Dynamic hydrology. McGraw-Hill, New York

Gabellani S, Boni G, Ferraris L, von Hardenberg J, Provenzale A (2007) Propagation of uncertainty from rainfall to runoff: A case study with a stochastic rainfall generator. Adv Water Resour 30(10):2061–2071. https://doi.org/10.1016/j.advwatres.2006.11.015

Hohmann C, Kirchengast G, Sungmin O, Rieger W, Foelsche U (2021) Small catchment runoff sensitivity to station density and spatial interpolation: hydrological modeling of heavy rainfall using a dense rain gauge network. Water 13(10):1381. https://doi.org/10.3390/w13101381

Hou J, Wang N, Guo K, Li D, Jing H, Wang T, Hinkelmann R (2020) Effects of the temporal resolution of storm data on numerical simulations of urban flood inundation. J Hydrol 589:125100. https://doi.org/10.1016/j.jhydrol.2020.125100

Huang Y, Bárdossy A, Zhang K (2019) Sensitivity of hydrological models to temporal and spatial resolutions of rainfall data. Hydrol Earth Syst Sci 23(6):2647–2663. https://doi.org/10.5194/hess-23-2647-2019

Keppel RV, Renard KG (1962) Transmission losses in ephemeral stream beds. J Hydraul Div 88(3):59–68. https://doi.org/10.1061/jyceaj.0000734

Kim C, Kim D (2020) Effects of rainfall spatial distribution on the relationship between rainfall spatiotemporal resolution and runoff prediction accuracy. Water 12(3):846. https://doi.org/10.3390/w12030846

Krajewski WF, Lakshmi V, Georgakakos KP, Jain SC (1991) A Monte Carlo Study of rainfall sampling effect on a distributed catchment model. Water Resour Res 27(1):119–128. https://doi.org/10.1029/90wr01977

Li X, Huang S, He R, Wang G, Tan ML, Yang X, Zhang Z (2020) Impact of temporal rainfall resolution on daily streamflow simulations in a large-sized river basin. Hydrol Sci J 65(15):2630–2645. https://doi.org/10.1080/02626667.2020.1836374

Li X, Wang L, Zhou H, Wang Y, Niu K, Li L (2022) The compound effect of spatial and temporal resolutions on the accuracy of urban flood simulation. Comput Intell Neurosci 2022:1–12. https://doi.org/10.1155/2022/3436634

Lin R, Zheng F, Yi M, Duan H, Chu S, Deng Z (2022) Impact of spatial variation and uncertainty of rainfall intensity on urban flooding assessment. Water Resour Manag 36(14):5655–5673. https://doi.org/10.1007/s11269-022-03325-8

Liu Y, Li Z, Liu Z, Luo Y (2021) Impact of rainfall spatiotemporal variability and model structures on flood simulation in semi-arid regions. Stoch Env Res Risk Assess 36(3):785–809. https://doi.org/10.1007/s00477-021-02050-9

Lobligeois F, Andréassian V, Perrin C, Tabary P, Loumagne C (2014) When does higher spatial resolution rainfall information improve streamflow simulation? An evaluation using 3620 flood events. Hydrol Earth Syst Sci 18(2):575–594. https://doi.org/10.5194/hess-18-575-2014

Lopes VL (1996) On the effect of uncertainty in spatial distribution of rainfall on catchment modelling. CATENA 28(1–2):107–119. https://doi.org/10.1016/s0341-8162(96)00030-6

Lyu H, Ni G, Cao X, Ma Y, Tian F (2018) Effect of temporal resolution of rainfall on simulation of urban flood processes. Water 10(7):880. https://doi.org/10.3390/w10070880

Meselhe EA, Habib EH, Oche OC, Gautam S (2009) Sensitivity of conceptual and physically based hydrologic models to temporal and spatial rainfall sampling. J Hydrol Eng 14(7):711–720. https://doi.org/10.1061/(asce)1084-0699(2009)14:7(711)

Michaud JD, Sorooshian S (1994) Effect of rainfall-sampling errors on simulations of desert flash floods. Water Resour Res 30(10):2765–2775. https://doi.org/10.1029/94wr01273

Michelon A, Benoit L, Beria H, Ceperley N, Schaefli B (2021) Benefits from high-density rain gauge observations for hydrological response analysis in a small alpine catchment. Hydrol Earth Syst Sci 25(4):2301–2325. https://doi.org/10.5194/hess-25-2301-2021

Nicótina L, Alessi Celegon E, Rinaldo A, Marani M (2008) On the impact of rainfall patterns on the hydrologic response. Water Resour Res 44(12). https://doi.org/10.1029/2007wr006654

Ochoa-Rodriguez S, Wang LP, Gires A, Pina RD, Reinoso-Rondinel R, Bruni G, Ichiba A, Gaitan S, Cristiano E, van Assel J, Kroll S, Murlà-Tuyls D, Tisserand B, Schertzer D, Tchiguirinskaia I, Onof C, Willems P, ten Veldhuis MC (2015) Impact of spatial and temporal resolution of rainfall inputs on urban hydrodynamic modelling outputs: A multi-catchment investigation. J Hydrol 531:389–407. https://doi.org/10.1016/j.jhydrol.2015.05.035

Paschalis A, Fatichi S, Molnar P, Rimkus S, Burlando P (2014) On the effects of small scale space–time variability of rainfall on basin flood response. J Hydrol 514:313–327. https://doi.org/10.1016/j.jhydrol.2014.04.014

Pechlivanidis IG, McIntyre N, Wheater HS (2017) The significance of spatial variability of rainfall on simulated runoff: an evaluation based on the Upper Lee catchment. UK Hydrol Res 48(4):1118–1130. https://doi.org/10.2166/nh.2016.038

Pilgrim DH, Cordery I (1975) Rainfall temporal patterns for design floods. J Hydr Engrg Div, ASCE 101(1):81–95

Porcu E, Furrer R, Nychka D (2020) 30 Years of space–time covariance functions. WIREs Comput Stat 13(2). https://doi.org/10.1002/wics.1512

Rafieeinasab A, Norouzi A, Kim S, Habibi H, Nazari B, Seo DJ, Lee H, Cosgrove B, Cui Z (2015) Toward high-resolution flash flood prediction in large urban areas – Analysis of sensitivity to spatiotemporal resolution of rainfall input and hydrologic modeling. J Hydrol 531:370–388. https://doi.org/10.1016/j.jhydrol.2015.08.045

Sapriza-Azuri G, Jódar J, Navarro V, Slooten LJ, Carrera J, Gupta HV (2015) Impacts of rainfall spatial variability on hydrogeological response. Water Resour Res 51(2):1300–1314. https://doi.org/10.1002/2014wr016168

Schuurmans JM, Bierkens MFP (2007) Effect of spatial distribution of daily rainfall on interior catchment response of a distributed hydrological model. Hydrol Earth Syst Sci 11(2):677–693. https://doi.org/10.5194/hess-11-677-2007

Segond ML, Wheater HS, Onof C (2007) The significance of spatial rainfall representation for flood runoff estimation: A numerical evaluation based on the Lee catchment, UK. J Hydrol 347(1–2):116–131. https://doi.org/10.1016/j.jhydrol.2007.09.040

Senan S, Thomas J, Vema VK, Jainet PJ, Nizar S, Sivan S, Sudheer KP (2022) A study of the influence of rainfall datasets' spatial resolution on stream simulation in Chaliyar River Basin, India. J Water Clim Chang 13(12):4234–4254. https://doi.org/10.2166/wcc.2022.273

Shahidi M, Abedini MJ (2018) Optimal selection of number and location of rain gauge stations for areal estimation of annual rainfall using a procedure based on inverse distance weighting estimator. Paddy Water Environ 16(3):617–629. https://doi.org/10.1007/s10333-018-0654-y

Singh VP (2016) Handbook of applied hydrology, (2nd ed.). McGraw-Hill Education
Smith MB, Koren VI, Zhang Z, Reed SM, Pan JJ, Moreda F (2004) Runoff response to spatial variability in precipitation: an analysis of observed data. J Hydrol 298(1–4):267–286. https://doi.org/10.1016/j.jhydrol.2004.03.039
Soroush F, Abedini MJ (2019) Optimal selection of number and location of pressure sensors in water distribution systems using geostatistical tools coupled with genetic algorithm. J Hydroinf 21(6):1030–1047. https://doi.org/10.2166/hydro.2019.023
Stone JJ, Nichols MH, Goodrich DC, Buono J (2008) Long-term runoff database, Walnut Gulch Experimental Watershed, Arizona. United States. Water Resour Res 44(5). https://doi.org/10.1029/2006wr005733
Terink W, Leijnse H, Van Den Eertwegh G, Uijlenhoet R (2018) Spatial resolutions in areal rainfall estimation and their impact on hydrological simulations of a lowland catchment. J Hydrol 563:319–335. https://doi.org/10.1016/j.jhydrol.2018.05.045
Wilson CB, Valdes JB, Rodriguez-Iturbe I (1979) On the influence of the spatial distribution of rainfall on storm runoff. Water Resour Res 15(2):321–328. https://doi.org/10.1029/wr015i002p00321
Younger PM, Freer JE, Beven KJ (2009) Detecting the effects of spatial variability of rainfall on hydrological modelling within an uncertainty analysis framework. Hydrol Process 23(14):1988–2003. https://doi.org/10.1002/hyp.7341
Zhang J, Han D (2017) Assessment of rainfall spatial variability and its influence on runoff modelling: A case study in the Brue catchment, UK. Hydrol Process 31(16):2972–2981. https://doi.org/10.1002/hyp.11250
Zhang J, Han D, Song Y, Dai Q (2018) Study on the effect of rainfall spatial variability on runoff modelling. J Hydroinf 20(3):577–587. https://doi.org/10.2166/hydro.2018.129
Zhou W, Zhu Z, Xie Y, Cai Y (2021) Impacts of rainfall spatial and temporal variabilities on runoff quality and quantity at the watershed scale. J Hydrol 603:127057. https://doi.org/10.1016/j.jhydrol.2021.127057